Available online at www.sciencedirect.com
SCIENCE DIRECT
Journal of Catalysis 232 (2005) 302–317
JOURNAL OF CATALYSIS
www.elsevier.com/locate/jcat

Enhancement of decane-SCR-NO_x over Ag/alumina by hydrogen. Reaction kinetics and in situ FTIR and UV–vis study

P. Sazama [a], L. Čapek [a], H. Drobná [a], Z. Sobalík [a], J. Dědeček [a], K. Arve [b], B. Wichterlová [a,*]

[a] *J. Heyrovský Institute of Physical Chemistry, Academy of Sciences of the Czech Republic, CZ-182 23 Prague 8, Czech Republic*
[b] *Laboratory of Industrial Chemistry, Process Chemistry Group, Åbo Akademi University, Åbo, Finland*

Received 2 December 2004; revised 23 February 2005; accepted 4 March 2005

Available online 22 April 2005

Abstract

Decane-SCR-NO_x, oxidation of NO and decane by molecular oxygen, and these reactions enhanced by hydrogen over Ag/alumina were investigated by monitoring of gaseous product composition, surface intermediates (in situ FTIR), and the state of silver (in situ UV–vis) under realistic reaction conditions in the steady-state and transient modes. It has been shown that oxidation of NO or decane by oxygen is greatly affected by the presence of decane or NO. Monodentate nitrates are formed preferentially and are more reactive compared with the bidentate species. Oxidation of decane mostly yields surface acetates, and the presence of NO_x favors the formation of formates (acrylates). The reaction steps most enhanced by the addition of hydrogen to the SCR-NO_x reaction are the transformations of the intermediate –CN species into –NCO and oxidation of the hydrocarbon to formates (acrylates). Although NO–NO_2 oxidation is also enhanced by hydrogen, this effect does not contribute to the increased rate of the SCR-NO_x reaction. A small part of very reactive Ag^+ (estimated to be $< 5\%$) is reduced to metallic charged $Ag_n^{\delta+}$ clusters ($n \leqslant 8$) during both the decane- and H_2/decane-SCR-NO_x reactions. The number of $Ag_n^{\delta+}$ clusters formed depends mainly on the level of NO conversion to nitrogen, regardless of whether the conversion level is attained by the addition of hydrogen or by an increased concentration of decane or oxygen in the feed. The time-resolved responses of NO_x–N_2 conversion and of the number of $Ag_n^{\delta+}$ clusters to the addition/removal of hydrogen from the reactants indicate that the $Ag_n^{\delta+}$ clusters are mainly formed because of the reducing effect of adsorbed CH_xO-containing reaction intermediates. The active sites are suggested to be single Ag^+ ions or small Ag_2O species. Hydrogen itself takes part in the SCR-NO_x reaction. It is supposed that it dissociates, forms Ag-hydride, and enhances SCR-NO_x by initiation radical reactions.

Keywords: Ag/alumina; SCR-NO_x; Hydrogen effect; Ag clusters; In situ FTIR; In situ UV–vis

1. Introduction

Among numerous catalysts screened for the selective catalytic reduction of NO_x to molecular nitrogen by hydrocarbons (CH_x-SCR-NO_x) under lean-burn conditions, Ag/alumina exhibits high activity at temperatures of 620–770 K, even in real exhaust gases. Nevertheless, in the low temperature range from 470 K, important for NO_x abatement from the exhaust gases of diesel-type engines, the conversion of NO to nitrogen is negligible [1–4]. Recently, a patent awarded to Daimler–Chrysler [5] and the results of Satokawa [6] described a dramatic positive effect of the addition of hydrogen to hydrocarbons on the conversion of NO_x to nitrogen over Ag/alumina catalysts, in the low-temperature range (400–620 K). The positive effect of hydrogen as a coreductant to hydrocarbons over Ag/alumina was reported for methane, C_2 and C_3 paraffins and olefins, isobutane [6–9], octane [5,10], and ammonia [11]. The "hydrogen effect" was also observed for Ag-ZSM-5 [12,13], but not for Ag supported on other carriers, such as silica, zirconia, and titania [7]. These findings indicate a specific state of Ag on alumina, and probably some contribution of alumina itself to the reaction [14].

* Corresponding author.
E-mail address: wichterl@jh-inst.cas.cz (B. Wichterlová).

0021-9517/$ – see front matter
doi:10.1016/j.jcat.2005.03.013

So far, the origin of the effect of hydrogen on the CH_x-SCR-NO_x reaction is a matter of discussion. The Satokawa and Hattori [8] groups revealed that the addition of hydrogen also affects the individual reaction steps, that is, the rate of oxidation of NO to NO_2 and of hydrocarbons to acetates and other intermediates. They concluded from in situ FTIR experiments that the rate-determining step of the C_3H_8-SCR-NO_x reaction is the formation of acetates, where the rate is enhanced by hydrogen, whereas the increase in NO–NO_2 conversion due to hydrogen co-assistance is not important for the overall SCR-NO_x process. Richter et al. [9] assumed that molecular oxygen dissociates over small Ag^0 clusters, formed by hydrogen reduction of appropriately sized Ag_2O clusters, and promotes oxidation of hydrocarbons to acetates and other oxygenates.

Another mechanism of SCR-NO_x over Ag/alumina was suggested by Bion et al. [16]. In the SCR-NO_x reaction with the use of ethanol, they found the formation of surface –CN groups bound to Ag^+, which they assumed to be interconverted into –NC entities and, in a subsequent step, further oxidized to –NCO groups. The latter surface intermediates were expected to react with another type of N-containing compound to molecular nitrogen in a final step.

Various types of Ag^+ cationic sites have been proposed as the active sites for the CH_x-SCR-NO_x reaction: isolated Ag^+ ions [16], small Ag-aluminate "clusters" [17], or Ag_2O species [9]. It was assumed that metallic Ag species yield N_2O and hydrocarbon combustion. In contrast, the positive effect of added hydrogen on the SCR-NO_x reaction was attributed exclusively to the formation of small charged metallic $Ag_n^{\delta+}$ clusters [6–8,12,13]. Satokawa et al. [12] first reported the appearance of the bands at 260 and 284 nm in the UV–vis spectrum of Ag-ZSM-5 (ascribed to small $Ag_n^{\delta+}$ clusters), exclusively after the C_3H_8-SCR-NO_x reaction performed with the co-assistance of hydrogen. Small $Ag_n^{\delta+}$ clusters with $n = 2$–4 were also revealed in Ag-ZSM-5 by ex situ EXAFS measurements [13] carried out after the H_2/C_3H_8-SCR-NO_x reaction. It was suggested that the $Ag_4^{\delta+}$ cluster is the active site in the presence of hydrogen [12,13].

We attempted to analyze the low-temperature (around 500 K) effect of added hydrogen on decane-SCR-NO_x over Ag/Al_2O_3 catalyst and on the individual reaction steps with respect to the reaction kinetics and changes in both the state of silver and surface reaction intermediates in the catalytic reactions. Decane has been chosen as a main component of diesel fuel. The analysis was based on monitoring both of the products in the gaseous phase and of the in situ UV–vis and FTIR spectra at various $H_2/C_{10}H_{22}/NO/O_2$, $H_2/NO/O_2$, and $H_2/C_{10}H_{22}/O_2$ feed compositions under the reaction conditions.

2. Experimental

2.1. The catalyst and its reducibility

Alumina-supported silver catalyst (1.76 wt% Ag) was prepared by impregnation of a commercial alumina with silver nitrate solution (< 250 μm; LaRoche) [4]. Temperature-programmed reduction by hydrogen was carried out with a Zeton Altamira AMI-200 under the following conditions: sample weight, 0.1 g (calcined at 720 K prior to measurements); heating rate, 20 K min^{-1}; flow rate of hydrogen in argon, 30 cm^3 min^{-1}.

2.2. Catalytic tests

A fixed-bed flow-through quartz microreactor was used to investigate the catalyst activity in the $C_{10}H_{22}$-SCR-NO_x and hydrogen-co-assisted $H_2/C_{10}H_{22}$-SCR-NO_x reactions, and in H_2, NO, and decane oxidation by molecular oxygen. The composition of the gases at the inlet of the reactor was typically 1000 ppm NO or NO_2, 300 ppm n-$C_{10}H_{22}$, 6% O_2, 0 or 12% H_2O, and 0–4000 ppm H_2. The weight of the catalyst (0.3–0.5-mm grains) was 210 mg, and the flow rate was 150 cm^3 min^{-1}, if not stated otherwise, corresponding to a GHSV of 30,000 h^{-1}. Prior to each catalytic test, the catalyst was calcined in an oxygen stream at 720 K for 1 h. The reactions of hydrogen, NO, and decane oxidation were carried out at concentrations and for contact times similar to those used for the SCR-NO_x reaction under the conditions given in the figures.

The concentrations of NO and NO_2 were monitored with a NO/NO_x chemiluminescence analyzer (Horiba CLA-355K), enabling determination of NO_x in the presence of a high concentration of water vapor. The concentrations of N_2, N_2O, H_2, CO, CO_2, and hydrocarbons were determined by an on-line connected Hewlett-Packard 6090 gas chromatograph. Two gaseous samples were injected with two 10-port valves. Columns of Poraplot Q and Molecular sieve 5A were used for the separation of O_2, N_2, H_2, CO_2, CO, and N_2O. A Poraplot Q column separated CO_2 from O_2, N_2, H_2, CO, and N_2O, and a six-port valve was used to bypass the column with Molecular sieve 5A during the analysis of CO_2. In the second branch, C_1–C_{10} hydrocarbons were separated on a nonpolar HP-5 column.

2.3. Diffuse-reflectance UV–vis–NIR in situ experiments

UV–vis–NIR spectra were collected on a Perkin-Elmer Lambda 19 UV–vis–NIR spectrophotometer, with the use of a diffuse-reflectance attachment with an integrating sphere coated with $BaSO_4$ and $BaSO_4$ as a reference. The absorption intensity was calculated from the Schuster–Kubelka–Munk equation, $F(R_\infty) = (1 - R_\infty)^2/2R_\infty$. A heated "home-made" flow-through quartz optical cell was used to obtain the spectra under the conditions of the catalytic reactions. The in situ UV–vis–NIR measurements were made at

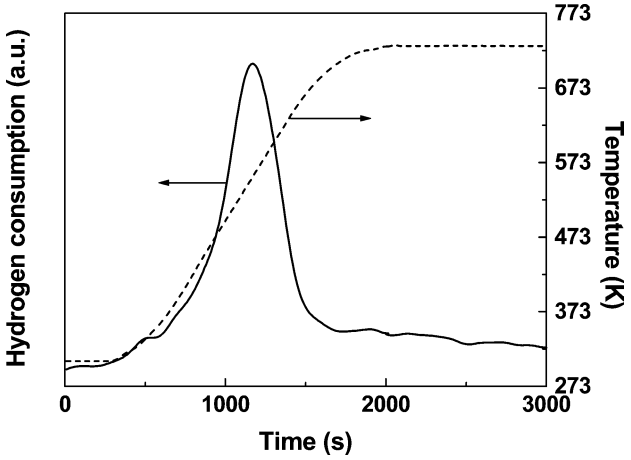

Fig. 1. H_2-TPR of Ag/Al_2O_3 catalyst.

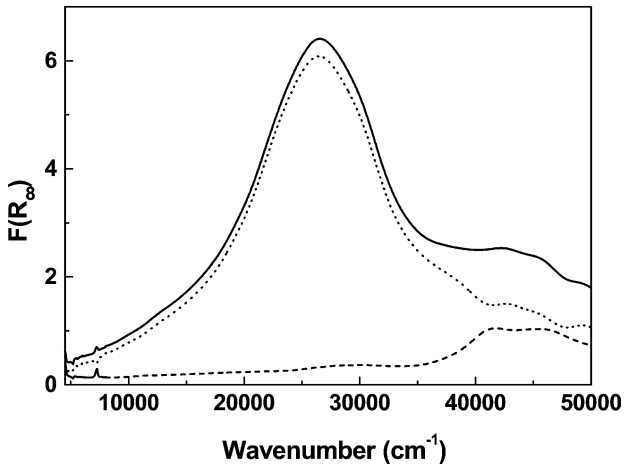

Fig. 2. In situ UV–vis–NIR spectra of reduced Ag/Al_2O_3 in H_2 flow at 520 K, when $\frac{1}{4}$ of Ag^+ content was reduced to metal. Spectrum of oxidized (––) and reduced (—) Ag/Al_2O_3. Difference spectrum (···).

temperatures of 470–570 K, and under the same conditions of reactant compositions and GHSV values as the catalytic tests.

2.4. FTIR in situ experiments

The catalyst, in the form of a thin, self-supporting wafer (ca. 10 mg cm^{-2}), was placed in a stainless-steel flow-through IR cell reactor (In-Situ Research Instruments, Inc.) with CaF_2 windows. The catalyst was calcined at 723 K in a stream of oxygen in helium for 1 h before all of the experiments and then cooled to the reaction temperature. Reactant mixtures were fed at a total flow rate of 17 cm^3 min^{-1} (GHSV approximately 43,000 h^{-1}). FTIR spectra were measured with a resolution of 2 cm^{-1} on a Nexus 670 e.s.p. FTIR spectrometer (Thermo Nicolet Co.) with a DTGS KBr detector. The spectrum of the calcined sample (recorded in a stream of oxygen at a given temperature) was subtracted from the monitored spectra recorded for the catalytic reaction.

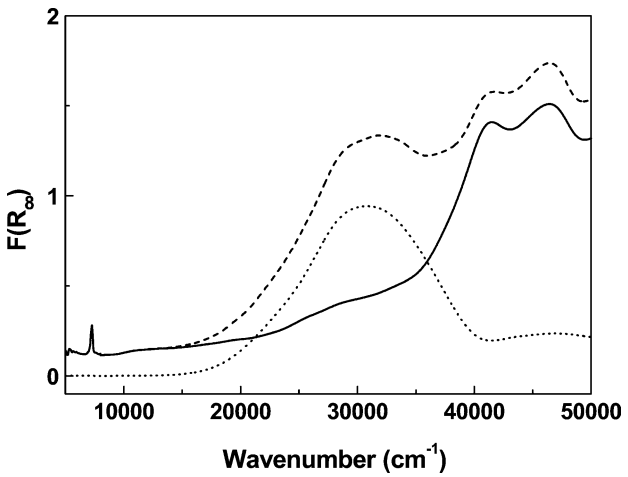

Fig. 3. Ag clusters formation at hydrogen oxidation over Ag/Al_2O_3. In situ UV–vis–NIR spectra of Ag/Al_2O_3 at 470 K in flow of O_2 (—) and under reaction conditions: 2000 ppm H_2 and 6% O_2 (––). Difference spectrum (···).

3. Results

3.1. Reduction of Ag/alumina by hydrogen

A single broad peak of hydrogen consumption, at TPR-H_2 centered at 540 K and corresponding to the reduction of Ag^+ to Ag^0, was registered up to 700 K (Fig. 1). Slightly less than approximately 50% of Ag^+ was reduced to the metallic state up to this temperature and even at prolonged heating, that is, within the temperature range employed for most of the catalytic tests. Further reduction of Ag^+ took place above 870 K.

Fig. 2 depicts in situ UV–vis spectra for Ag/alumina in an oxygen stream and reduced at 520 K in hydrogen. According to the hydrogen consumption, roughly a quarter of the silver was reduced at this temperature. Whereas the oxidized sample exhibited bands at 41,600 and 46,600 cm^{-1} assigned to the electronic transition of isolated Ag^+ ions, after its reduction with hydrogen at 520 K an intensive broad band centered at 26,000 cm^{-1} appeared. This absorption reflects the formation of various metallic charged $Ag_n^{\delta+}$ clusters and Ag particles (see below). The high intensity of absorption indicates an extremely high extinction coefficient for this metallic silver compared with those of Ag^+ ions. But as various clusters and particles are formed, the overall band intensity, reflecting various Ag species, cannot be used for quantitative analysis.

3.2. Hydrogen oxidation by molecular oxygen

At a temperature of 470 K and for the feed composition given in Fig. 3, nearly complete conversion of H_2 was achieved, and a strong broad band centered at approximately 31,000 cm^{-1} indicated the formation of small charged $Ag_n^{\delta+}$ clusters (for UV–vis band attribution see the

Discussion). Surprisingly, with development of the broad band at 31,000 cm^{-1} during hydrogen oxidation, the original intensity of the bands of Ag^+ ions at 41,600 and 46,000 cm^{-1} did not change. When at 520 K hydrogen conversion was complete, no $Ag_n^{\delta+}$ clusters (31,000 cm^{-1}) were observed, and the spectrum exhibited only the bands of Ag^+ ions at 41,600 and 46,600 cm^{-1}. It should be mentioned that the reduction of silver in Ag/alumina occurred in hydrogen (10 kPa) under mild conditions already at room temperature (RT). The well-separated UV–vis bands at 28,000 and 34,000 cm^{-1} (not shown in the figure), corresponding to some small $Ag_n^{\delta+}$ clusters, appeared and increased in intensity with increasing time of Ag/alumina exposure to hydrogen.

3.3. *Effect of hydrogen on NO oxidation with molecular oxygen*

Oxidation of NO to NO_2 over Ag/alumina practically did not proceed at 470 K, but the conversion of NO to NO_2 was strongly enhanced by hydrogen addition, as already reported in [7], regardless of whether water vapor (12%) was present or absent in the feed. Without hydrogen, the NO/O_2 mixture over Ag/alumina at 470 K yielded only adsorbed NO_x species (Fig. 4A). For interpretation of IR spectra see Table 1. The predominant nitrite species were bridging nitrites, $(M–O)_2{=}N$, with a band at 1230 cm^{-1}, and chelating nitro compounds, $M_2–O–N–O$, with a shoulder at 1180 cm^{-1}, on Ag/Al_2O_3 and parent Al_2O_3 (Figs. 4A and B, respectively). The intensities of the nitrite bands are slightly higher over the alumina surface, probably because of blocking of the alumina surface adsorption sites by the Ag^+ species. In accordance with the kinetic results indicating acceleration of the $NO + O_2$ reaction at 470 K after H_2 addition over Ag/Al_2O_3 and Al_2O_3, formation of both mono- (1245 cm^{-1}) and bidentate (1295 cm^{-1}) surface nitrates was observed (Fig. 4). Taking into consideration the much lower degree of NO_2 formation in the gas phase over Al_2O_3, an almost identical intensity of nitrate species was obtained over both Ag/Al_2O_3 and Al_2O_3. This is consistent with the decrease in the adsorption capacity of the Ag/alumina surface for the adsorption of nitrates, because of Ag^+ ions bound to the alumina.

Replacement of NO/O_2 with NO_2 feed (identical NO_x concentration) leads to an increase in the total intensity of the IR nitrate bands of nearly sevenfold over Al_2O_3, whereas this value would remain nearly the same over Ag/Al_2O_3 (Fig. 5). Thus, based on the changes in the intensity of the nitrate bands, it could be assumed that, on fully oxidized Ag/Al_2O_3, over 90% of the sorption capacity of the parent alumina is blocked for NO_2 adsorption. Then the small increase in nitrate formation produced by H_2 addition to the NO_2 stream (Fig. 5) could be explained by assuming partial reduction of Ag^+. Based on the intensity of the nitrates adsorbed in the absence and presence of H_2 in the NO_2 stream,

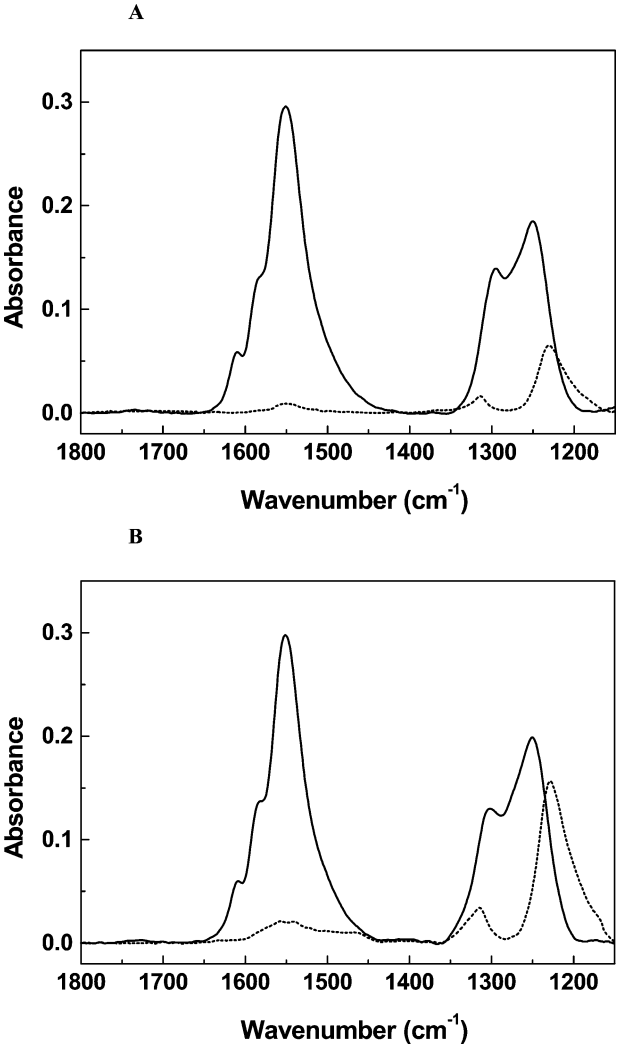

Fig. 4. FTIR spectra of adsorbed species in flow of 1000 ppm NO and 6% O_2 on Ag/Al_2O_3 (A) and Al_2O_3 (B) in the presence (—) and absence (···) of 1000 ppm H_2.

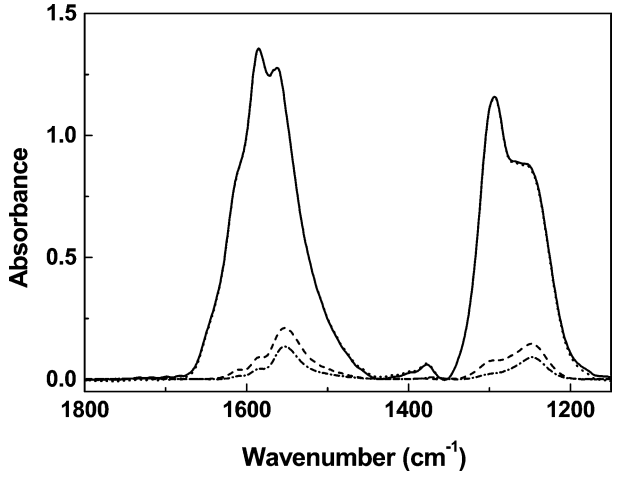

Fig. 5. FTIR spectra of adsorbed species in flow of 1000 ppm NO_2 on Ag/Al_2O_3 in the presence (—) and absence (···) of 1000 ppm H_2 and on Al_2O_3 in the presence (– –) and absence (–·–) of 1000 ppm H_2.

Table 1
Assignment of the FTIR bands observed on Ag/Al_2O_3 and alumina

	Surface species	IR bands (cm^{-1})		Refs.
		Reference	Experiment	
NO_x species	Free NO_3^- ion	1380		[20]
	Monodentate nitrate	1530–1480, 1290–1250	1550, 1245	[20,29]
	Bidentate nitrate	1565–1500, 1300–1260	1590, 1295	[20,29]
	Bridging nitrate	1650–1600, 1225–1170	Missing	[20]
	Free NO_2^- ion	1260, 1330		[20]
	Bridging nitrite	1220–1205	1230	[20]
	M–NO_2 nitro	1440–1335		[20]
	Chelating nitro	1520–1390, 1260–1180	1180	[20]
	Adsorbed NO_x	1560	1560	[27]
CHO species	Carboxylate COO^-	1585, 1460		[27]
	Acetate	1578, 1466	1578–1580, 1457	[16]
	Formate $HCOO^-$	3005–3000, 2910–2907, 1595–1589, 1393–1391	1390, 1373	[15,16,27]
	Carbonate	1639, 1270		[8]
	CH_x	3100–2800	3000–2800	[28]
	Acrylate on Ag/Al_2O_3	1642–1645, 1572–1580, 1456–1461, 1378–1392, ∼1300	1390, 1373	[18]
N–C species	Al(VI)–NCO	2255		[16]
	Al(IV)–NCO	2228	2230–2250	[16]
	Ag/or Al–CN	2155, 2127	2150	[16]

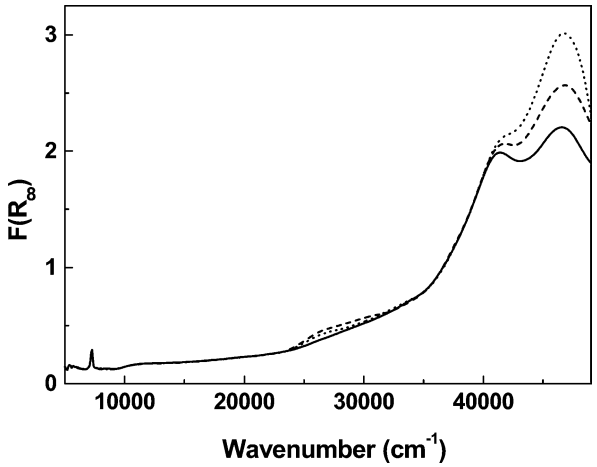

Fig. 6. In situ diffuse reflectance UV–vis spectra of Ag/Al_2O_3 at 523 K in flow of O_2 (—) and under reaction conditions: 1000 ppm NO, 6% O_2, without H_2 (– –) and with 2000 ppm H_2 (···).

about 5% of the Ag^+ present would be reduced to Ag^0, thus leaving some of the alumina adsorption sites free.

The in situ UV–vis spectra recorded at NO/O_2 and $H_2/NO/O_2$ at 470 K show a very low increase in the absorbance intensity in the 25,000–35,000 cm^{-1} range due to hydrogen addition (Fig. 6). It reflects the appearance of a negligible number of $Ag_n^{\delta+}$ clusters (cf. Fig. 2). An increase in the intensity of absorbance above 42,000 cm^{-1} with a maximum at 47,000 cm^{-1} following hydrogen addition can be explained by the formation of adsorbed nitrates.

3.4. Effect of hydrogen on decane oxidation by molecular oxygen

Whereas only a low acceleration of the rate of decane oxidation due to hydrogen addition at 470 K was obtained in the kinetic test (not shown in the figure), the increase in the coverage of the surface CH_x species with hydrogen addition was appreciable; note that the FTIR spectra were monitored in the absence of water vapor in the feed (see Fig. 7). The positive hydrogen effect on decane oxidation is reflected by a high increase in the intensity of the acetate bands at 1457, 1578, and 1320 cm^{-1}, and to a lesser extent, of the formate (acrylate) species (1390 and 1373 cm^{-1}) (see Table 1). An increase in the bands in the CH_x region (3000–2800 cm^{-1}) could not be assigned to the $–CH_3$ groups of acetates [18]. This indicates increased accumulation of hydrocarbon species in the presence of hydrogen without a significant change in their composition. Thus hydrogen only accelerates the general trends in the decane oxidation by molecular oxygen with the same patterns of transformation.

3.5. Effect of hydrogen on $C_{10}H_{22}$-SCR-NO_x

Fig. 8 demonstrates the high promotion effect of hydrogen in the $C_{10}H_{22}$-SCR-NO reaction over Ag/Al_2O_3, particularly at low temperatures (< 620 K), as already reported for other paraffins and olefins as well as ammonia [6–11]. But hydrogen alone did not yield nitrogen. The enhancement effect of hydrogen for the $C_{10}H_{22}$-SCR-NO reaction was also reflected in the higher conversion of decane to carbon oxides, but without a significant change in the CO yields above 370 K. In the low-temperature region (470–620 K),

the conversion of NO to N_2O was increased slightly (up to 10%) in the presence of hydrogen. At higher temperatures (> 620 K), it had a tendency to decrease and became negligible. The positive hydrogen effect on $C_{10}H_{22}$-SCR-NO at high space velocities is also remarkable; at 570 K hydrogen co-assistance yielded NO conversions of 50 and 30% at GHSV of 120,000 and 240,000 h^{-1}, respectively.

If water vapor was not fed into the $H_2/C_{10}H_{22}$-SCR-NO_x reaction, slow but substantial deactivation of the catalyst took place (Fig. 9). After 300 min, the NO conversion decreased to the values similar to those obtained in the reaction carried out without hydrogen as a coreductant. Thus, a concentration of water vapor of 12% in the stream (like that present in the real exhausts of diesel engines) is valuable, as it prevents catalyst deactivation. Similar deactivation was observed in decane oxidation by molecular oxygen. This implies that water vapor suppresses the adsorption of various hydrocarbons and their derivates and thus "cleans" the catalyst surface.

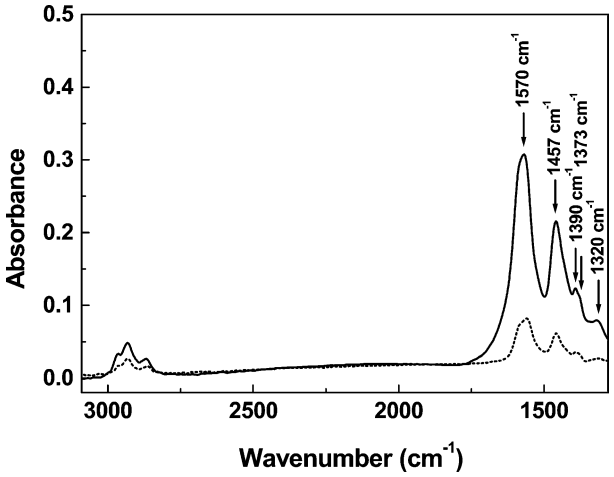

Fig. 7. FTIR spectra of adsorbed species at 473 K in flow of $C_{10}H_{22}$ (750 ppm) and O_2 (6%) on Ag/Al_2O_3, in the presence (—) and absence (···) of H_2 (1000 ppm).

3.6. Effect of NO vs. NO_2 on $C_{10}H_{22}$- and $H_2/C_{10}H_{22}$-SCR-NO_x

To elucidate the effect of NO_2 on the $C_{10}H_{22}$-SCR-NO_x reaction and the reaction co-assisted by hydrogen (both reactions carried out in 12% water vapor), NO was partly or completely replaced by NO_2 in the reactant feed (Table 2). It is clearly seen that the higher concentrations of NO_2 at low temperatures decreased the conversion of NO_x to N_2 for SCR-NO, for both decane and decane co-assisted by hydro-

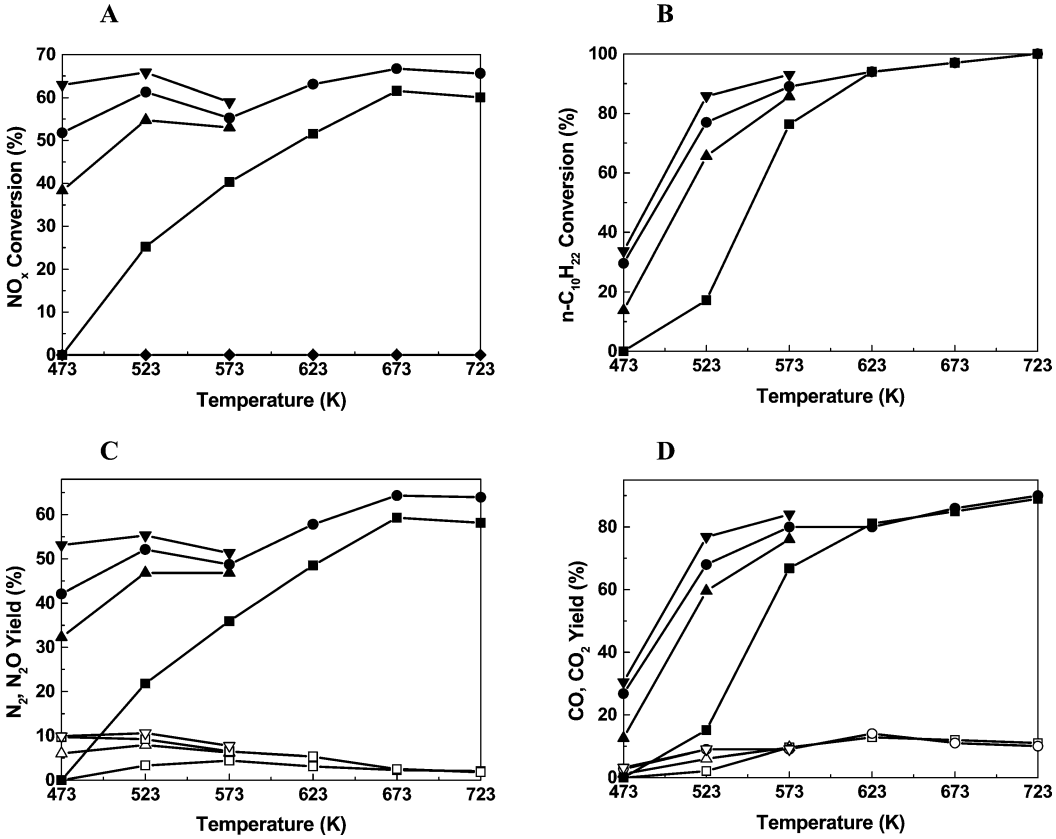

Fig. 8. Effect of hydrogen on $C_{10}H_{22}$-SCR-NO over Ag/Al_2O_3 depending on temperature. Feed: 1000 ppm NO, 300 ppm $C_{10}H_{22}$, 6% O_2, 12% H_2O and 0 ppm H_2 (■,□), 1000 ppm H_2 (▲,△), 2000 ppm H_2 (●,○), 4000 ppm H_2 (▼,▽) and 2000 ppm H_2, 0 ppm $C_{10}H_{22}$ (◆). Yield of N_2 and CO_2 (solid points) and yield of N_2O and CO (open points).

Table 2
Effect of hydrogen on $C_{10}H_{22}$-SCR-NO_x over Ag/Al_2O_3

NO_x feed	473 K				523 K			
	0 ppm H_2		2000 ppm H_2		0 ppm H_2		2000 ppm H_2	
	NO_x (%)	$C_{10}H_{22}$ (%)	NO_x (%)	$C_{10}H_{22}$ (%)	NO_x (%)	$C_{10}H_{22}$ (%)	NO_x (%)	$C_{10}H_{22}$ (%)
1000 ppm NO	0	0	18.4	11.9	9.7	8.5	64.8	47.0
500 ppm NO + 500 ppm NO_2	~1	~1	13.0	11.5	3.9	5.6	54.4	42.3
1000 ppm NO_2	~1	~1	8.6	10.0	1.6	4.2	44.3	41.7

Conditions: 1000 ppm NO_x, 500 ppm $C_{10}H_{22}$, 6% O_2, 12% H_2O, and 0 and 2000 ppm H_2. GHSV = 60,000 h^{-1}.

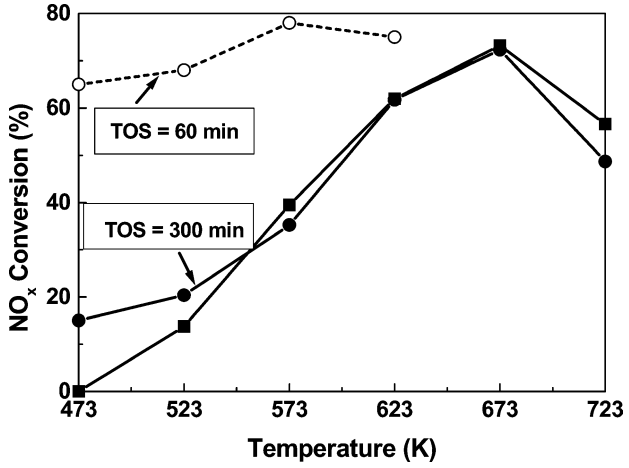

Fig. 9. Effect of hydrogen and deactivation in the water vapor absence in $H_2/C_{10}H_{22}$-SCR-NO on temperature over Ag/Al_2O_3. Feed: 1000 ppm NO, 300 ppm decane, 6% O_2, 0% H_2O, 2000 ppm H_2 (●,○) or 0 ppm H_2 (■).

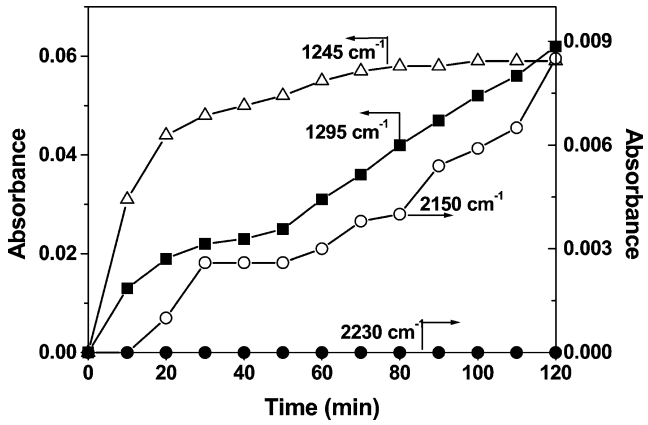

Fig. 10. Dependence of intensities of the IR bands characteristic for monodentate nitrates (1245 cm^{-1}), bidentate nitrates (1295 cm^{-1}) and –CN species (2150 cm^{-1}) on T-O-S. In situ decane-SCR-NO: NO (1000 ppm), O_2 (6%), decane (750 ppm) in the absence of hydrogen over Ag/Al_2O_3 at 473 K.

gen. It is also shown that hydrogen enhanced the rate of the SCR-NO_2 reaction.

3.7. Effect of hydrogen on the surface intermediates in $C_{10}H_{22}$-SCR-NO_x

The previous kinetic results yield the specification of conditions under which the reaction system is transformed from the "initial" stage of adsorbed reactants and intermediates (without the production of the gaseous products) to the progress of the catalytic reaction, exclusively by the addition of hydrogen to the feed. The process of deactivation of the Ag/Al_2O_3 catalyst performing in "dry" SCR-NO_x reaction streams (cf. Fig. 9) and the uncertainty in the identical GHSV values in the IR cell and in the microreactor tests preclude quantitative correlation with the rates found in the microreactor. Nevertheless, the general trends in NO and CH_x conversions in the SCR-NO_x reaction at 470 K caused by hydrogen addition are quite obvious. The IR frequencies attributed to surface reaction species according to the literature are given in Table 1.

3.7.1. Surface intermediates in the SCR-NO_x mixtures without hydrogen

Nitrite surface forms, occurring in the NO/O_2 mixture, were not found in significant amounts on the surface of Ag/alumina in the SCR-NO reaction at 470 K, but nitrates were formed. Whereas the monodentate form (band at 1245 cm^{-1}) was formed preferentially and attained a constant value with time, the intensity of the bidentate nitrate (1295 cm^{-1}) increased slowly but steadily (Fig. 10). Accordingly, formation of surface nitrates in the $C_{10}H_{22}/NO/O_2$ mixture at 470 K, which were nearly absent with the NO/O_2 feed, must be accelerated by a hydrocarbon or its oxidation products (see Fig. 10). The presence of NO_x would also substantially accelerate $C_{10}H_{22}$ conversion into adsorbed formate (acrylate) species (cf. spectra taken in the absence of hydrogen, Figs. 11A and 7) in comparison with its oxidation by molecular oxygen when acetates predominate. A weak band at about 2150 cm^{-1} (Fig. 11A) also indicates the formation of –CN species in the $C_{10}H_{22}/NO/O_2$ mixture. However, no –NCO species (2230–2250 cm^{-1}) were identified at 470 K without hydrogen.

This implies that in the initial stages of the SCR-NO_x reaction the surface is covered by nitrates, products of $C_{10}H_{22}$ activation (bands around 2900 cm^{-1}), formates (acrylates) (1390 and 1373 cm^{-1}), and, to a small extent, acetates (1457, 1578, and 1320 cm^{-1}). Formation of all of these species is accelerated by the presence of both reaction components, NO_x and decane.

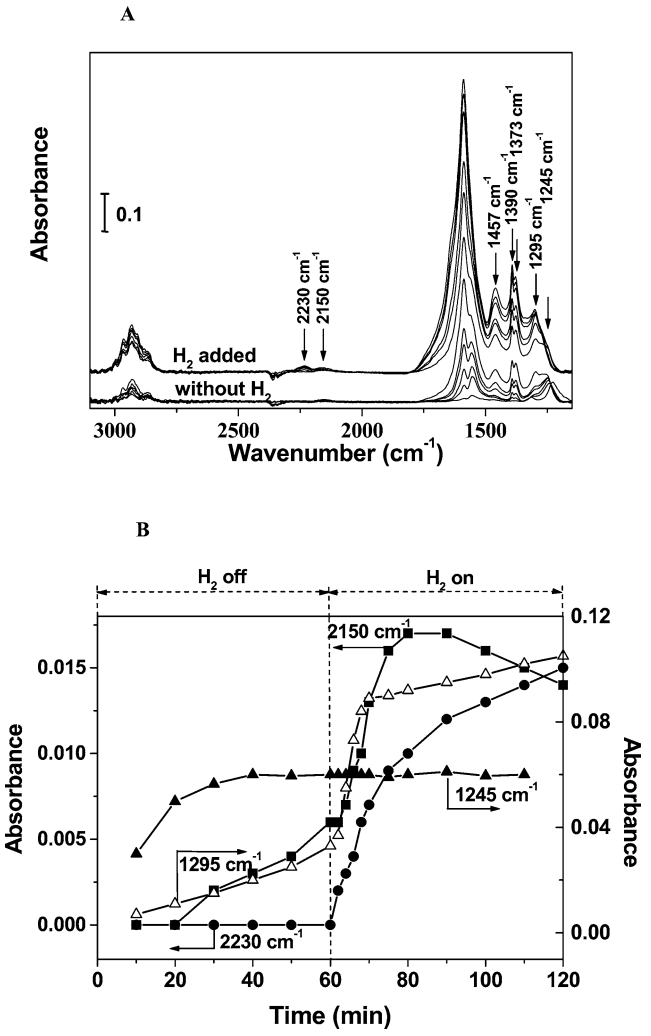

Fig. 11. In situ FTIR spectra of decane-SCR-NO in the presence and absence of hydrogen on Ag/Al_2O_3 at 473 K. (A) Development of FTIR spectra of adsorbed species with T-O-S, and (B) evolution of intensities of the bands characteristic for adsorbed species (monodentate nitrates 1245 cm^{-1}, bidentate nitrates 1295 cm^{-1}, –CN 2150 cm^{-1} and –NCO 2230 cm^{-1}). Feed: NO (1000 ppm), O_2 (6%), decane (750 ppm), 0 or 1000 ppm H_2.

3.7.2. Surface intermediates in the SCR-NO_x reaction accelerated by hydrogen

The addition of hydrogen accelerates all of the previously described surface processes. The IR bands of the nitrate and carboxyl species reached the steady-state values in the $H_2/C_{10}H_{22}/NO/O_2$ mixture. Bidentate nitrate species responded to the presence of hydrogen with an increase in concentration, which is further stabilized. On the other hand, only the concentration of monodentate species apparently did not respond to the addition of hydrogen, as they were simultaneously fast consumed by their further transformation. The rate of formation of –CN species bound to Ag^+ ions (2150 cm^{-1}) was also increased considerably because of the presence of hydrogen, but most significantly –NCO species (2230 cm^{-1}, bound on Al^{3+}) appeared and steeply increased.

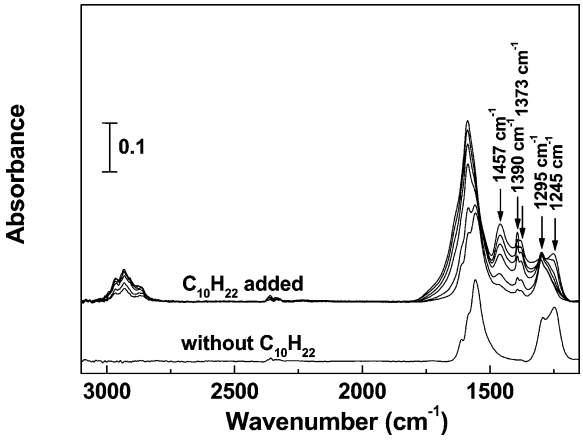

Fig. 12. In situ FTIR spectra of the reaction of pre-adsorbed NO_2 ($NO_2/O_2/H_2$) with decane (750 ppm) at 473 K on Ag/Al_2O_3 in the presence of H_2.

To elucidate the effect of the individual reactant components on the formation of the individual intermediates, experiments were carried out in the presence of hydrogen with pre-adsorption of NO_2 or decane. The NO_2 pre-adsorption at 470 K for the $H_2/NO_2/O_2$ mixture would provide the characteristic profile of the monodentate and bidentate nitrate species (Fig. 12). When we switched from the $H_2/NO_2/O_2$ stream to the $H_2/C_{10}H_{22}/O_2$ mixture, the intensity in the CH_x region quickly reached levels exceeding those for $H_2/C_{10}H_{22}/O_2$ activation, and both carboxyl species increased and reached ratios typical for $C_{10}H_{22}$ activation in the presence of NO_x. The response of the individual nitrate species was basically different. The monodentate responded through a steep decrease, but the bidentate form was nearly stable, indicating the much higher reactivity of the monodentate form. The rate of formation of both –CN and –NCO species was low after exposure of the surface to pre-adsorbed NO_x and to the decane mixture. Pre-adsorption of the $H_2/C_{10}H_{22}/O_2$ mixture at 470 K produced acetate (bands at 1580 and 1457 cm^{-1}) and a much lower amount of formate (acrylate) species (1390 and 1374 cm^{-1}; see Fig. 13), as also followed from the IR spectrum (reaction without hydrogen) shown in Fig. 7. Replacing decane with NO-containing feed ($H_2/NO/O_2$) would greatly accelerate production of the formate (acrylate) species, whereas the intensity of the acetate band (1457 cm^{-1}) would not be substantially changed from that attained with the $H_2/C_{10}H_{22}/O_2$ mixture. Thus, the acetate species proved to be rather stable in the NO_x-containing feed under the given reaction conditions. In accordance with the demonstrated important role of NO_x in formate (acrylate) production, this species was nearly absent after the pre-adsorption step, but its amount increased substantially after we switched to the NO_x-containing stream. Both –CN and –NCO species were formed after the NO_x addition. In comparison with steady-state conditions, a relatively high intensity of –NCO groups was attained.

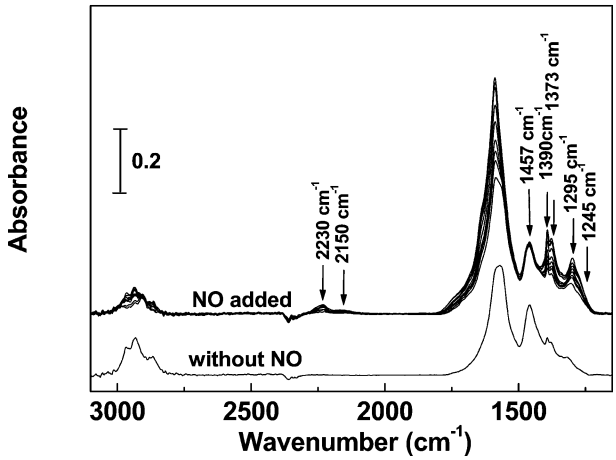

Fig. 13. In situ FTIR spectra of the reaction of pre-adsorbed decane (750 ppm decane/O_2H_2) with NO (1000 ppm) at 473 K on Ag/Al_2O_3 in the presence of hydrogen (1000 ppm).

3.8. *Effect of hydrogen, decane, and oxygen on the state of silver in $C_{10}H_{22}$-SCR-NO*

Fig. 14 depicts the in situ UV–vis–NIR spectra of Ag/Al_2O_3 at 520 K in an oxygen stream, in the $C_{10}H_{22}$-SCR-NO reaction and the reaction with added hydrogen; note that all of the experiments were carried out in the presence of water vapor (12%). Whereas, in an oxygen stream, the bands of Ag^+ ions at 41,600 and 46,600 cm^{-1} were detected (only very low absorption is around 30,000 cm^{-1}), in the $C_{10}H_2/NO/O_2$ stream at 520 K, where conversion of NO to N_2 was observed (see Fig. 14C), an intensity increase of the absorbance at approximately 27,000–38,000 cm^{-1} and in the range 42,000–50,000 cm^{-1} appeared (see Figs. 14A and B). Absorption in the former range indicates the formation of very low number of small $Ag_n^{\delta+}$ clusters. Addition of hydrogen (1000–4000 ppm) to the reaction mixture caused a substantial increase in conversions of NO_x to nitrogen, and decane to CO_x, predominantly to CO_2, and a slight increase in the yield of nitrous oxide (Figs. 14C and D). The UV–vis spectra clearly indicate that the favorable effect of hydrogen on the conversions of NO and decane was accompanied by a dramatic increase in the spectrum intensity in the region from approximately 20,000 to 40,000 cm^{-1}, with a broad maximum centered at approximately 31,000 cm^{-1}, and an intensity increase in the 42,000–50,000 cm^{-1} region. The positions of the individual bands forming the envelope of the broad band with a maximum around 31,000 cm^{-1} were estimated from the derivation mode of the subtracted spectra (Fig. 14B). The maxima were identified at approximately 27,000, 31,000, and 38,000 cm^{-1}. Increasing the

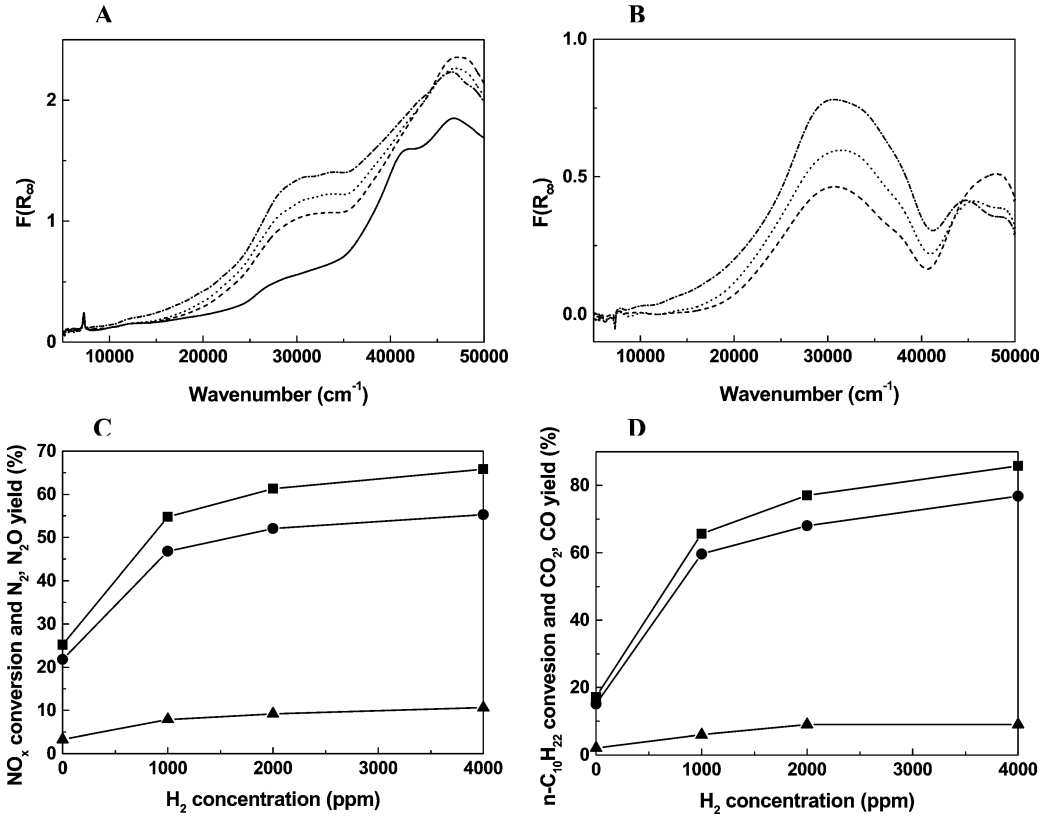

Fig. 14. Effect of hydrogen concentration on decane-SCR-NO over Ag/Al_2O_3 at 523 K. Feed: 1000 ppm NO, 300 ppm $C_{10}H_{22}$, 6% O_2, 12% H_2O and 0–4000 ppm H_2. (A) In situ diffuse reflectance UV–vis–NIR spectra of Ag/Al_2O_3 in flow of O_2 (—) and under reaction conditions: without H_2 (– –), with 1000 ppm H_2 (···) and with 2000 ppm H_2 (–·–). (B) Difference spectrum between that under reaction conditions and the spectrum in flow of O_2. (C or D) NO_x or $C_{10}H_{22}$ conversion (■), N_2 or CO_2 yield (●) and N_2O or CO yield (▲).

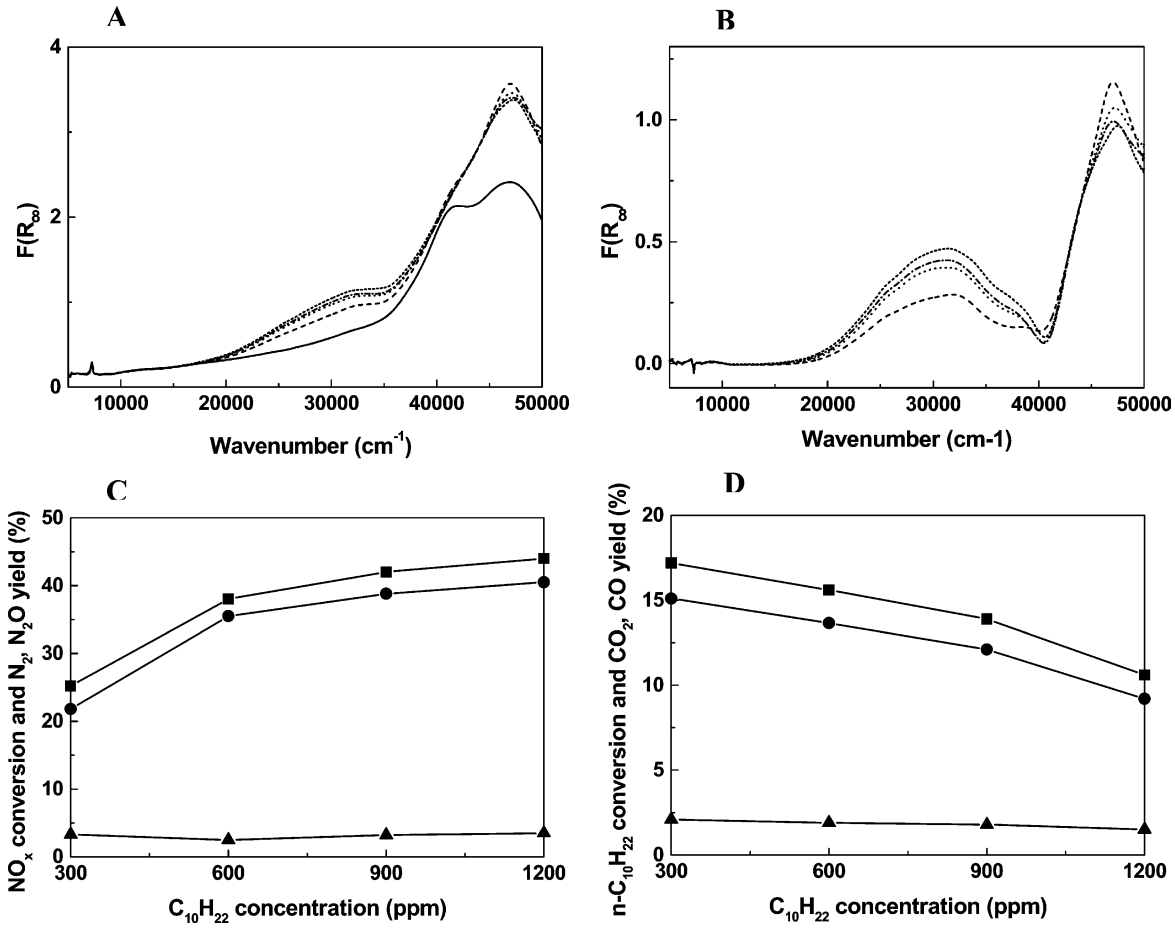

Fig. 15. Effect of decane concentration on decane-SCR-NO at 523 K. Feed: 1000 ppm NO, 6% O_2, 12% H_2O, and 300–1200 ppm $C_{10}H_{22}$. (A) In situ diffuse reflectance UV–vis–NIR spectra of Ag/Al_2O_3 in flow of O_2 (—) and under reaction conditions: with 300 ppm decane (– –), 600 ppm decane (· · ·), 900 ppm decane (–·–) and with 1200 ppm decane (- - -). (B) Difference spectrum between that under reaction conditions and the spectrum in flow of O_2. (C or D) NO_x or $C_{10}H_{22}$ conversion (■), N_2 or CO_2 yield (●), and N_2O or CO yield (▲).

concentration of the added hydrogen resulted in higher NO_x conversions and higher intensity of the broad absorption, without a significant shift in the wavenumbers; only the low-intensity tail at low wavenumbers was more pronounced for Ag/alumina under the reaction conditions, exhibiting the highest NO conversion. This development of the shape of the spectrum indicates that small charged $Ag_n^{\delta+}$ clusters, probably of similar dimensions, increase in concentration, but larger metallic species are formed only to a very low degree. The intensity increase of absorption ranging from 42,000 to 50,000 cm^{-1} could be connected with adsorbed nitrates, detected in the IR spectra. Moreover, this suggestion is supported by the spectral behavior given in Figs. 14A–16A, where the intensity of this absorption is affected by oxidation of NO to NO_2 and by consumption of NO_2 in the SCR-NO_x reaction. As the composition and concentration of NO_x vary depending on the reaction conditions, and their bands overlap those of Ag^+ ions, their details will not be discussed here.

With increasing decane concentration at $C_{10}H_{22}$-SCR-NO_x, conversion of NO_x increased, particularly between 300 and 600 ppm decane (Fig. 15), but the yields of N_2O and CO were not affected. Simultaneously with increasing concentrations of decane, the intensity of the broad band around 31,000 cm^{-1} and of the absorbance at 42,000–50,000 cm^{-1} also increased. A similar effect was found with increasing oxygen concentration (Fig. 16). Conversions of NO_x and decane increased especially between 3 and 6% oxygen concentration in the feed, and the N_2O yield also increased. Surprisingly, this favorable effect of oxygen was also accompanied by an increase in the intensity of the broad absorbance (31,000 cm^{-1}) of $Ag_n^{\delta+}$ clusters, and by a substantial intensity increase in the range of 42,000–50,000 cm^{-1}, attributed to the formation of adsorbed NO_x species.

Thus, the increasing concentrations of both decane and oxygen in the $C_{10}H_{22}$-SCR-NO_x reaction resulted in increasing conversion of NO to nitrogen and an increasing intensity of the broad band roughly at the same wavenumbers, around 27,000, 31,000, and 38,000 cm^{-1}. Even at high oxygen concentrations and high amounts of adsorbed nitrates, there is clear evidence for the occurrence of a significant number of $Ag_n^{\delta+}$ clusters in the Ag/alumina catalyst.

To estimate the relative rates of change in NO_x conversion and formation of $Ag_n^{\delta+}$ clusters in the presence of

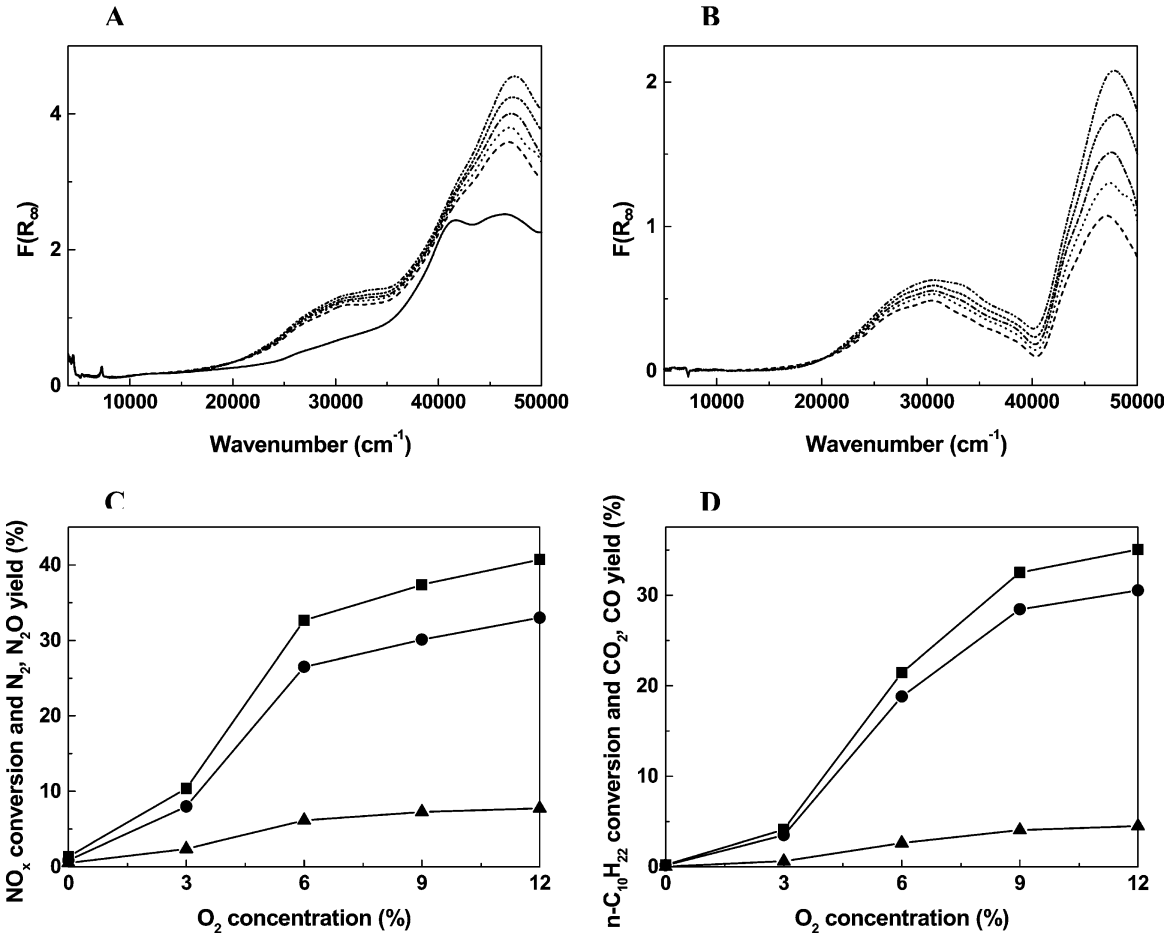

Fig. 16. Effect of oxygen concentration on decane-SCR-NO at 523 K. Feed: 1000 ppm NO, 600 ppm $C_{10}H_{22}$, 12% H_2O, and 0–12% O_2. (A) In situ diffuse reflectance UV–vis–NIR spectra of Ag/Al_2O_3 in flow of O_2 (—) and under reaction conditions: without O_2 (– –) and with 3% O_2 (· · ·), 6% O_2 (–·–), 9% O_2 (- - -) and 12% O_2 (·····). (B) Difference spectrum between that under reaction conditions and the spectrum in flow of O_2. (C or D) NO_x or $C_{10}H_{22}$ conversion (■), N_2 or CO_2 yield (●), and N_2O or CO yield (▲).

hydrogen, time-resolved experiments of hydrogen switching on/off in the $C_{10}H_{22}$-SCR-NO reaction at 523 K were performed (Fig. 17). The NO_x consumption increased sharply within seconds after H_2 addition, with the peak of NO_x consumption followed by stabilization of the NO_x concentration. Switching off hydrogen caused an opposite, slightly longer response (within 4 min) in the NO_x concentration. These experiments showed complete reversibility in NO_x conversion values in the absence and presence of hydrogen in the feed. The existence of a peak in NO_x consumption after hydrogen addition is explained by enhanced NO_2 adsorption due to the presence of hydrogen (cf. Fig. 4A).

The addition of hydrogen to the $C_{10}H_{22}$-SCR-NO mixture, inducing fast NO_x consumption, was accompanied by a rather similar pattern in the increase in the absorbance with a maximum around 31,000 cm^{-1} (Fig. 17A), and the rate of increase in the band intensity was only slightly lower compared with changes in the NO_x concentration. On the other hand, when the hydrogen was switched off, a fast drop in the NO_x conversion with hydrogen elimination (Fig. 17B) did not result in a similar rate of decrease in the number of $Ag_n^{\delta+}$ clusters. It was evidently several orders slower. This implies that there is no straightforward relationship between the rate of change in the NO_x conversion and the number of small charged $Ag_n^{\delta+}$ clusters present under the reaction conditions.

4. Discussion

Although the positive effect of hydrogen over Ag/alumina for the CH_x-SCR-NO_x reactions was demonstrated for a spectrum of hydrocarbons, it is worth pointing out that with decane, the main component of diesel engine exhausts, a similar hydrogen effect has been observed. The conversion of NO to nitrogen was enhanced dramatically, predominantly at low a temperature range (470–620 K) and at extremely high space velocities (up to 240,000 h^{-1}). Both of these ranges of conditions are essential for NO_x abatement in diesel engine exhausts. During the H_2-assisted $C_{10}H_{22}$-SCR-NO_x reaction, the presence of a high excess of water vapor in the gas stream is beneficial with respect to the long-term catalyst operation, since, without water vapor in the stream, a substantial decrease in the NO_x conversion to

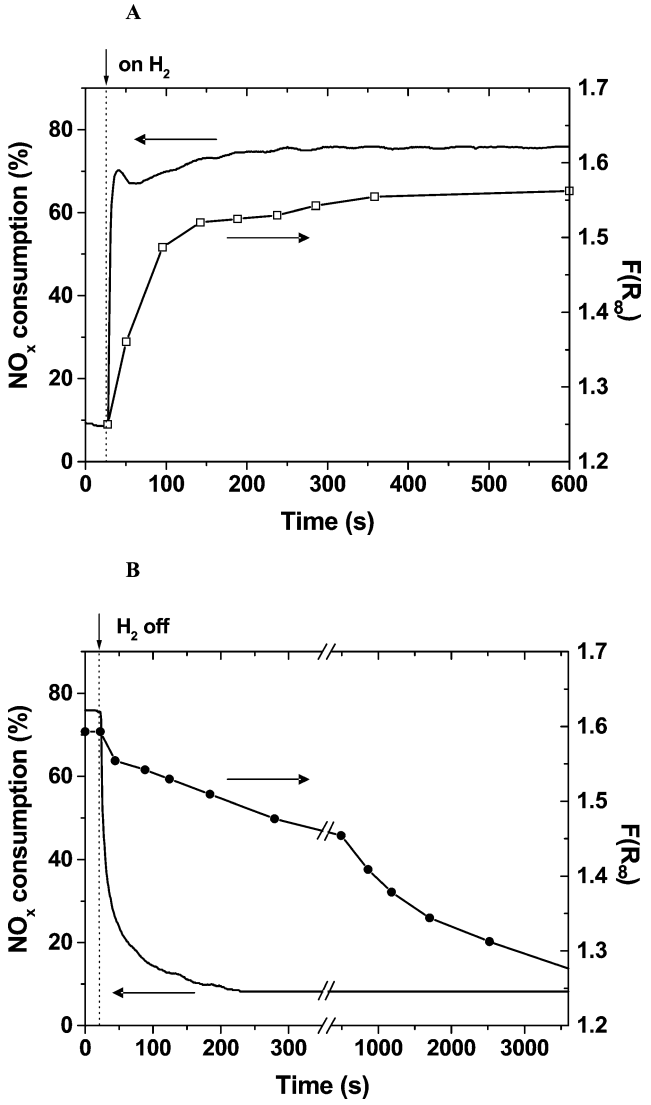

Fig. 17. Effect of hydrogen switching on/off in decane-SCR-NO over Ag/Al_2O_3 at 523 K, 1000 ppm NO, 600 ppm decane, 6% O_2 and 0 or 2000 ppm H_2. GHSV = 60,000 h^{-1}. NO_x consumption and intensity of the UV–vis band at 31,000 cm^{-1} as a function of time and hydrogen switch (A) on and (B) off.

nitrogen with time occurs because of the formation of deposits adsorbed to the catalyst surface (see Fig. 9). These deposits are represented by olefin-type intermediates, as decane readily cracks with the formation of olefins, which have a tendency to oligomerize at low temperatures.

Contrary to the highly beneficial effect of hydrogen on NO conversion, its presence slightly increases yields (up to 10%) of undesired N_2O and CO, especially at low temperatures (470–570 K) (Fig. 8). The appearance of N_2O in the products might indicate the participation of the NO decomposition mechanism over the metallic silver, similar to the mechanism occurring on Pt-based catalysts [1]. Formation of minor concentration of metallic silver could not be excluded, as some absorption below 25,000 cm^{-1} is detected in UV–vis spectra (see, e.g., Fig. 14B). However, it should be noted that under conditions leading to increasing concentration of NO_2 (i.e., at increasing hydrogen and oxygen concentration in the feed at SCR-NO_x), formation of N_2O is enhanced, whereas variation of decane concentration has no effect on the N_2O yield. This finding, in contrast, might indicate the incomplete reduction of NO_x to nitrogen without the participation of the NO decomposition mechanism. The effect of NO_2 on the reduction of NO_x to nitrogen over Ag/alumina catalysts for the SCR-NO_x process is reported controversially in the literature. Both a positive [14] and a negative [7,9] effect of NO_2 were found compared with NO. Bethke and Kung [14] have shown that enhancement of the conversion of NO_x to nitrogen by NO_2 with propane as a reductant also depends on the Ag loading on alumina. In our case with decane, it is clearly shown (Table 2) that the rate of SCR-NO_x for relatively high concentrations of NO_2 is lower compared with that observed when NO is used. Shimidzu et al. [17] explained the lower NO_x conversions with NO_2 at low temperature by strong adsorption of nitrates. Therefore, the different results might be connected with the type of hydrocarbon and the reaction conditions used.

However, without any doubt hydrogen enhances the rate of oxidation of NO to NO_2 at low temperatures (470–520 K) (see Fig. 4 and [7]) and thus leads to an increased concentration of NO_2 in the gas phase and a pool of nitrates on the surface. But as the high concentration of NO_2 in the feed results in lower N_2 yields, the positive effect of hydrogen on the NO_x conversion to nitrogen in the $C_{10}H_{22}$-SCR-NO_2 reaction (Table 2) could not generally be accounted for by enhancement of the reaction of oxidation of NO to NO_2. Thus, another function of hydrogen, reflected rather in hydrocarbon oxidation, could contribute to the enhanced SCR-NO_x activity.

4.1. Surface intermediates in SCR-NO_x over Ag/alumina enhanced by hydrogen

The surface intermediates formed in the NO/O_2, $C_{10}H_{22}/O_2$, and $C_{10}H_{22}/NO/O_2$ reactions over Ag/alumina at 470 K (at in situ conditions), when the products have still not evolved into the gas phase, could be assumed to reflect the initial steps in the mechanistic pathways. Propagation of these reactions by the addition of hydrogen to the reactant streams, reflected in the formation of gaseous products and thus a dramatic increase in conversions of NO and decane, is manifested by a different population of the individual surface intermediates.

In the presence of hydrogen, nitrites are immediately transformed into nitrates in NO/O_2 and SCR-NO_x mixtures (Fig. 4). Of the surface nitrates, the monodentate type is clearly preferably formed, and it reacts much faster with CH_x compared with the bidentate type (Fig. 11). This is why monodentate nitrates do not increase their surface concentrations after hydrogen addition. In the $C_{10}H_{22}/NO/O_2$ feed composition, they are transformed into cyanides, which represent the final intermediate product at 470 K in the absence

Table 3
Band positions for various silver species in UV–vis spectra

Wavenumber (cm^{-1})	Ag species	Comments	Refs.
32,300	Ag_2^+	Mordenite	[22]
37,700	Ag_4^{2+}	Mordenite	[22]
39,200, 32,800	Ag_4^{2+}	ZSM-5	[13]
30,300	Ag_5^0	Mordenite	[22]
34,500	$Ag_7^{\delta+}$ or $Ag_8^{\delta+}$	Mordenite	[22]
30,800	$Ag_8^{\delta+}$	Solution, magic cluster	[26]
31,300	Ag_8^0	Mordenite	[22]
28,200	$(Ag_4^+)_2$	Mordenite	[22]
25,600–27,000	$Ag_n^{\delta+}$ ($n = 2$–7)	γ-Al_2O_3, SiO_2	[21]
34,500–37,000	$Ag_n^{\delta+}$ ($n = 2$–7)	γ-Al_2O_3, SiO_2	[21]
42,600, 47,600	Ag^+	ZSM-5	[13]
44,400, 47,600, 52,100	Ag^+	$Ag(H_2O)_4$	[19]
41,700	Ag^+	γ-Al_2O_3, SiO_2	[21]
44,600, 47,200, 51,000	Ag^+	ZSM-5	[23]
52,600	Ag^+	ZSM-5	[24]
From NIR to UV region	Ag_2O	Bulk	[25]
41,600, 46,600	Ag^+	γ-Al_2O_3	This study
27,000, 28,000, 30,000, 31,000, 34,000, 38,000	$Ag_n^{\delta+}$ ($n \leqslant 8$)	γ-Al_2O_3	This study
ca. < 26,000	Ag agglomerates	γ-Al_2O_3	This study

of hydrogen. In the absence of hydrogen the complete absence of –NCO species at 470 K indicates that the –CN to –NCO reaction might be the rate-determining step.

It should be stressed that there is a dramatic difference in the surface intermediate composition in the oxidation of decane by oxygen and by the NO/O_2 mixture or by preadsorbed NO_2 (cf. Figs. 12 and 13). Whereas surface acetates dominate in CH_x oxidation by molecular oxygen, the presence of NO_2 clearly favors the formation of formates (acrylates) in both cases, that is, in the presence and absence of hydrogen. This is in contradiction to SCR-NO_x with propane, where the predominant surface intermediates, enhanced by addition of hydrogen, were reported to be acetates [8]. On the other hand, Iglesias-Juez et al. [18], investigating propene-SCR-NO_x over Ag/alumina, found among organic surface species a prevailing concentration of surface acrylates. These results point out the differences caused by using paraffins or olefins in the SCR-NO_x reaction. As already mentioned above, in our case decane cracks to lower chain olefins and paraffins. More reactive olefins can then be expected to be involved in the reaction with NO_x.

The addition of hydrogen as a co-reductant to decane enhances all of these steps in the SCR-NO_x process, leading to various types and concentrations of surface intermediates. The hydrogen effect on the surface intermediates is predominantly manifested in the enhanced transformation of –CN to –NCO (see Fig. 11) and the formation of predominant formates (acrylates) over acetates. As proposed already by Bion et al. [16], the transformation of silver cyanide into alumina-bonded isocyanate species seems to be the slowest step of the mechanism of similar SCR-NO_x by ethanol over the Ag/alumina catalyst.

In addition to these clearly manifested favorable effects of hydrogen on the SCR-NO_x reaction in the transformation of –CN to –NCO and CH_x to formates (acrylates), the positive effect of hydrogen on the transformation of NO to NO_2 need not be beneficial under all circumstances for the NO_x conversion to N_2, as high concentrations of NO_2 in the feed at low temperature result in lower NO_x conversions to N_2 (see Table 2). Nevertheless, the observed increase in the rate of nitrate formation and fast consumption predominantly of the monodentate type in the presence of hydrogen indicate that the transformation of NO to NO_2 is enhanced not only in the NO/O_2 reaction but also in decane-SCR-NO_x. This implies that the SCR-NO_x reaction evidently proceeds not via nitrites, but via surface nitrates reacting with CH_x.

4.2. Ag species operating in the SCR-NO_x reactions

4.2.1. UV–vis spectra of Ag species

The electronic spectra of silver in solutions, inert gas-solid matrices, and zeolites show that Ag^+ ions and small Ag clusters exhibit characteristic absorption bands in the UV–vis region. It is widely accepted that the components of the UV bands above 40,000 cm^{-1} correspond to $4d^{10} \rightarrow 4d^9 5s^1$ electronic transitions of Ag^+ ions in the various matrices [19], and the bands between 30,000 and 40,000 cm^{-1} were ascribed to the $4d^{10}5s^1 \rightarrow 4d^9 5s^1 5p^1$ and $4d^{10}5s^1 \rightarrow 4d^9 5s^1 6p^1$ transitions in Ag_n clusters with $n \leqslant 8$ [21,22]. The assignment of the individual bands to silver species given in the literature and in this study is summarized in Table 3. There is no doubt that the observed UV absorption bands at 41,600 and 46,600 cm^{-1} correspond to the isolated Ag^+ ions. However, there is clear evidence that not all of the

Ag^+ ions are quantitatively reflected in these bands. In contrast to the $4d^{10} \rightarrow 4d^9 5s^1$ transitions below 49,000 cm^{-1} reported for various solids, the spectrum of Ag^+ ions can be also reflected in the region above 50,000 cm^{-1}, and, moreover, the absorption in this region can be dominant [19]. This was observed in aqueous Ag^+ ion solutions [19] and recently in Ag-ZSM-5 [23,24]. Thus some types of Ag^+ ions can be "invisible" for UV–vis spectroscopy. The possibility of the presence of the spectral component above 50,000 cm^{-1} in the Ag/alumina sample is indicated by an increase in the absorbance around 50,000 cm^{-1} for some experiments (see, e.g., Fig. 3).

The absence of a significant decrease in the spectrum intensity of Ag^+ ions between 40,000 and 50,000 cm^{-1} when $Ag_n^{\delta+}$ clusters are formed could be explained by very high differences in extinction coefficients for Ag^+ ions and $Ag_n^{\delta+}$ clusters, as follows from Fig. 2, or by the occurrence of the Ag^+ $4d \rightarrow 5s$ transitions above 50,000 cm^{-1}. From a comparison of the intensity of the broad band of small Ag clusters when a quarter of Ag^+ ions were reduced (Fig. 2) with that monitored during the SCR-NO_x reaction, it follows that roughly only $< 5\%$ of Ag^+ was reduced. This implies that a minor part (either detected or undetected) of Ag^+ ion species is highly reactive and can easily be reduced and transformed under various conditions to a variety of metal Ag clusters. This finding might support speculation about the presence of silver in the form of Ag_2O in Ag/alumina, as suggested in [9]. However, the characteristic absorption of bulk Ag_2O and Ag_2O thin layers, exhibiting absorption from NIR to the UV region [25], was not observed in the oxidized Ag/alumina sample.

In conclusion, the UV–vis spectra cannot provide a quantitative picture of the behavior of all of the Ag^+ ions in alumina under the reaction conditions. Nevertheless, the results of UV–vis spectroscopy with the TPR experiments suggest assignment of the UV absorption bands at 41,600 and 46,600 cm^{-1} to Ag^+ ions in an oxygen ligand environment, the vast amount of which does not undergo changes in the valence state, at least up to 750 K, that is, up to the temperature of the investigated SCR-NO_x process. It can be speculated that these Ag^+ ions represent silver aluminate species that are resistant to reduction. A low number of silver clusters is formed either from the Ag^+ ions detected by absorption bands at 41,600 and 46,600 cm^{-1} or originates from undetected Ag^+ ions. Such Ag^+ ions can represent single ions or very small (Ag_2O) species.

In contrast, the UV–vis spectra measured under true in situ reaction conditions have provided more detailed insight into the development of small $Ag_n^{\delta+}$ clusters, depending on the reaction conditions, although this approach also suffers from some limitations. The nature and size of the metal-type $Ag_n^{\delta+}$ clusters, to which are ascribed bands below 40,000 cm^{-1} in the spectra of Ag/alumina, are still under discussion (see Table 3). The EXAFS experiments permitted direct identification of cluster size in zeolites only up to four Ag atoms (see [12,13]). The surrounding local field of silver in zeolites is different from that affecting Ag clusters on the alumina support. Moreover, in the case of zeolites, strong guest-host interaction between the Ag species and the framework can also be accompanied by spatial restrictions, as shown, for example, in [22].

Pestryakov and Davydov [21] attributed the bands found with Ag/Al_2O_3 at 34,000–36,000 cm^{-1} and 25,000–27,000 cm^{-1} to small Ag_n clusters ($n = 2$–7) with s–s* and n–s* electron transitions, respectively. As they observed a strong donor–acceptor interaction between the Ag^+ ions and the alumina carrier when using adsorbed CO, they suggested the induction of an effective charge on silver clusters with the formation of $Ag_n^{\delta+}$ species. The absorption observed for the Ag/alumina sample in the 30,000–32,000 cm^{-1} region can be attributed to $Ag_8^{\delta+}$ clusters, as these were monitored by direct-mass spectrometric experiments, in aqueous solutions [19] and in the confined space of zeolites [7,22]. The presence of $Ag_8^{\delta+}$ clusters is supported by the fact that Ag clusters exhibiting the same UV–vis spectrum contain Ag atoms with three nearest neighbors in the first coordination sphere, that is, $Ag_4^{\delta+}$ clusters with tetrahedral symmetry or $Ag_8^{\delta+}$ clusters with cubic symmetry. The presence of $Ag_8^{\delta+}$ clusters is more probable because of their significantly higher stability (magic clusters) compared with $Ag_4^{\delta+}$ clusters, which are extremely unstable [26].

4.2.2. Ag species under the reaction conditions

In very mild reduction of silver in the Ag/Al_2O_3 sample under vacuum, as well as at low hydrogen pressure at RT, the bands monitored at 28,000 and 34,000 cm^{-1} can be ascribed to the $Ag_n^{\delta+}$ clusters. Under the conditions of the $H_2 + O_2$ reaction over Ag/alumina, these two characteristic bands were no longer resolved, and the existence of a broad band ranging from 20,000 to 40,000 cm^{-1} (with a half-width ranging from 24,600 to 37,400 cm^{-1}) indicated the presence of several types of small $Ag_n^{\delta+}$ clusters, which are hard to define with respect to their nuclearity. Bearing in mind the relatively high stability of silver clusters with $n = 8$, under the conditions of Ag/alumina reduction, the observed local maximum of absorption around 31,000 cm^{-1}, in addition to the maxima at 28,0000 and 34,000 cm^{-1} for $Ag_n^{\delta+}$ clusters, can probably be ascribed to the presence of $Ag_n^{\delta+}$ clusters with $n = 8$.

The shape of the UV–vis bands in the region from 20,000 to 40,000 cm^{-1} for $Ag_n^{\delta+}$ clusters observed during the $C_{10}H_{22}$-SCR-NO_x reaction or that co-assisted by hydrogen at various reactant/product compositions is much more complex. Nevertheless, as the shape of the broad band is not significantly varied, depending on reaction conditions and reactant compositions, it can be inferred that more or less similar $Ag_n^{\delta+}$ species are present in the catalyst active in the $H_2/C_{10}H_{22}$-SCR-NO_x reaction. It should be pointed out that under the reaction conditions investigated (with stable NO_x conversions for many hours), we did not observe the formation of large metallic Ag^0 particles, which should be manifested in strong absorption in the visual spectrum.

4.3. Effect of reactant composition and hydrogen on NO oxidation and CH_x-SCR-NO_x: state of Ag and surface intermediates

Based on the ex situ UV–vis spectra and EXAFS studies, analyzing the state of silver after the H_2/propane-SCR-NO_x reaction [12,13], the authors suggested that the positive "hydrogen effect" is caused by formation of small $Ag_n^{\delta+}$ clusters, with $n = 2$–4, in the Ag-ZSM-5 catalyst. Our results indicate that during the decane-SCR-NO_x reactions the most populated are probably $Ag_8^{\delta+}$ clusters, in addition to clusters of other nuclearity. With the NO–NO_2 reaction using similar NO and H_2 concentrations as those in the $C_{10}H_{22}$-SCR-NO_x reaction, only a very low, an apparently insignificant concentration of $Ag_n^{\delta+}$ clusters was formed, although the conversion of NO was increased dramatically (Fig. 6). This implies that either this extremely low number of $Ag_n^{\delta+}$ clusters is sufficient for enhancement of the NO–NO_2 reaction rate or the hydrogen function in the NO–NO_2 reaction is not connected with the function of these $Ag_n^{\delta+}$ clusters. In [9], dissociation of oxygen on small Ag clusters was assumed, but the experimental evidence was not provided. We speculate that the HO_2 radicals formed (see below) are responsible for NO to NO_2 oxidation at in the presence of hydrogen or hydrocarbon (cf. enhancement of NO–NO_2 oxidation by both hydrogen and decane; see Figs. 4 and 12, respectively).

Comparison of the UV–vis spectra for Ag/alumina in the H_2/$C_{10}H_{22}$-SCR-NO_x reaction at various feed compositions (cf. Figs. 14–16) indicates that, in both the presence and absence of hydrogen as co-reductant, small $Ag_n^{\delta+}$ clusters are present in the catalyst. Their number clearly increases with increasing conversion of NO to nitrogen, regardless of whether this conversion increase is achieved by an increase of the concentration of hydrogen or decane or even of oxygen. This finding implies that there is some obvious relationship (although not quantitative) between the conversion of NO to N_2 and the number of small $Ag_n^{\delta+}$ clusters in the catalyst. Hence the conversion of NO to N_2 also depends on the catalyst activity in the oxidation of NO and CH_x by molecular oxygen, and CH_x by NO_x; the relationship between the Ag structure and SCR-NO_x activity could not be easily established.

On the other hand, the system immediately responds (completely reversibly) to hydrogen addition and removal in increased and decreased NO conversion, respectively, and the responses in the changes in the number of small charged $Ag_n^{\delta+}$ clusters were substantially much slower (particularly at hydrogen removal from the reactant feed; see Fig. 17). It follows that the $Ag_n^{\delta+}$ clusters are not formed exclusively as a result of hydrogen addition, but that their number during the SCR-NO_x reaction is controlled mainly by the accumulation of surface organic intermediates (cf. data in Figs. 7, 10, and 11).

Therefore, the number of small $Ag_n^{\delta+}$ clusters can be related to the reducing environment present on the catalyst surface formed by the SCR-NO_x reaction in both cases, that is, in the presence and absence of hydrogen. Accordingly, the presence of $Ag_n^{\delta+}$ clusters is not the exclusive reason for the enhanced activity of Ag/alumina, but hydrogen itself has to take part in the reaction. In [30,31] it was shown that hydrogen dissociates when it adsorbs to Ag^+ in zeolites and generates acidic protons and silver hydride. Methane also dissociates on silver with formation of $CH_3^{\delta+}$ and silver hydride [30]. Similar processes of hydrogen dissociation and hydrocarbon activation might occur at SCR-NO_x over Ag/alumina. We speculate that silver hydride at the SCR reaction mixture immediately reacts with oxygen to form hydroperoxy radicals (HO_2)

$$\mathrm{Ag{-}H} + \mathrm{O_2} \rightarrow \mathrm{HO_2} + \mathrm{Ag^0}.$$

Hydroperoxy radical, which is a highly active oxidant [32], readily reacts with NO to NO_2 and hydroxyl radical [32,33] according to the following reaction:

$$\mathrm{HO_2} + \mathrm{NO} \rightarrow \mathrm{NO_2} + \mathrm{OH}.$$

Both of these radicals can react with hydrocarbons to their oxo/nitro derivates [32]. We suppose that hydrogen addition enhances the formation of silver hydride and thus supports radical-type reactions. Such a mechanism of hydrogen (and hydrocarbon) functioning is in accord with the experimental observations obtained in this study that both hydrogen and decane enhance NO–NO_2 oxidation, hydrogen enhances all of the SCR-NO_x reaction steps, and the occurrence of gas-phase radical-type transformations behind the catalyst bed was observed at octane-SCR-NO_x (without hydrogen) over Ag/alumina catalyst [4].

5. Conclusions

The study of decane-SCR-NO_x in the presence/absence of hydrogen over Ag/alumina showed that hydrogen substantially increases the conversion of NO to nitrogen, particularly in the low-temperature region (470–720 K) as well as at high space velocities (60,000–240,000 h^{-1}). Investigation of the reaction steps via surface intermediates and relevant catalyst structure under the conditions of the SCR-NO_x reaction (and the oxidation of NO and decane by molecular oxygen) over Ag/alumina catalyst at low temperatures (around 500 K) in the steady state and transient modes revealed that:

(i) The oxidation of NO or decane with oxygen is greatly affected by the presence of the second component, that is, decane or NO. With an NO/O_2 mixture (470 K), surface nitrites prevail. Oxidation of nitrites to nitrates is enhanced by the presence of both hydrogen and decane. Nitrate monodentate is formed preferentially, and it is more reactive compared with the bidentate species. Analogously, oxidation of decane with oxygen yields

mostly surface acetates, and the presence of NO_x favors the formation of formates and acrylates. However, hydrogen addition in decane oxidation with molecular oxygen, enhancing the concentration of surface intermediates, does not alter their composition and surface acetates prevail.

(ii) The surface reaction steps, which are enhanced most by the addition of hydrogen to the SCR-NO_x reaction, are transformation of intermediate –CN species, bound on Ag^+ into –NCO, connected with Al sites of alumina, and oxidation of decane to formates (acrylates).

(iii) Small metallic $Ag_n^{\delta+}$ clusters are formed in a significant but low number during the SCR-NO_x reaction, depending mainly on the degree of NO conversion to nitrogen, regardless of whether the conversion is increased by the addition of hydrogen or an increased concentration of decane or oxygen in the feed. Thus, there is an apparent correlation between the concentration of $Ag_n^{\delta+}$ clusters and the NO–N_2 conversion. However, a comparison of the time-resolved responses of the NO_x conversion values and the number of $Ag_n^{\delta+}$ clusters under the SCR-NO_x reaction clearly indicates that the $Ag_n^{\delta+}$ clusters are formed, besides by hydrogen, mainly through the reducing effect of adsorbed CH_x-O-containing reaction intermediates. The concentration of these sorbed intermediates and thus of $Ag_n^{\delta+}$ clusters increases with the increased rate of the SCR-NO_x reaction.

(iv) The active Ag^+ center participating in the reaction is represented by a single Ag^+ ion or very small Ag_2O species. A redox cycle at the SCR-NO_x reaction occurs between Ag^+ (Ag_2O) and $Ag_n^{\delta+}$ clusters (with $n \leqslant 8$) in both cases, in the absence and presence of hydrogen as co-reductant.

(v) It is concluded that the enhancement effect of hydrogen on SCR-NO_x is accompanied by the formation of an increased concentration of small $Ag_n^{\delta+}$ clusters, which, however, are already present on the catalyst during the decane-SCR-NO_x reaction. Acceleration of the SCR-NO_x reaction by hydrogen originates mainly from the increased rate of oxidation of hydrocarbons and of the –CN to –NCO reaction step, but not from the increased rate of the NO–NO_2 reaction. It is supposed that hydrogen itself participates in the SCR-NO_x reaction by dissociating with the formation of silver hydride, proton sites, and then hydroperoxy and hydroxy radical species. These radical species might dramatically enhance the propagation of the SCR-NO_x reaction.

Acknowledgments

The authors acknowledge financial support from the European Union via the Ammonore project G5RD2001-00595 and the Grant Agency of the Academy of Sciences of the Czech Republic through project T400400413.

References

[1] R. Burch, J.P. Breed, F.C. Meunier, Appl. Catal. B 39 (2002) 283.
[2] K. Eränen, L.-E. Lindfors, A. Niemi, P. Elfving, L. Cider, SAE paper 2000-01-2813 (2000).
[3] A. Martinez-Arias, M. Fernandez-Garcia, A. Iglesias-Juez, J.A. Anderson, J.C. Conesa, J. Soria, Appl. Catal. B 28 (2000) 29.
[4] K. Eränen, L.-E. Lindfors, F. Klingstedt, D.Yu. Murzin, J. Catal. 219 (2003) 25.
[5] B. Krutzsch, Ch. Goerigk, S. Kurze, G. Wenninger, W. Boegner, F. Wirbeleit, US Patent 5,921,076 (1999).
[6] S. Satokawa, Chem. Lett. (2000) 294.
[7] S. Satokawa, J. Shibata, K. Shimizu, A. Satsuma, T. Hattori, Appl. Catal. B 42 (2003) 179.
[8] J. Shibata, K. Shimizu, S. Satokawa, A. Satsuma, T. Hattori, Phys. Chem. Chem. Phys. 5 (2003) 2154.
[9] M. Richter, U. Bentrup, R. Eckelt, M. Schneider, M.-M. Pohl, R. Fricke, Appl. Catal. B 51 (2004) 261.
[10] K. Eränen, F. Klingstedt, K. Arve, L.-E. Lindfors, D.Yu. Murzin, J. Catal. 227 (2004) 328.
[11] M. Richter, R. Fricke, R. Eckelt, Catal. Lett. 94 (2004) 115.
[12] J. Shibata, Y. Takada, A. Shichi, S. Satokawa, A. Satsuma, T. Hattori, J. Catal. 222 (2004) 368.
[13] J. Shabata, K. Shimidzu, Y. Takada, A. Shichi, H. Yoshida, S. Satokawa, A. Satsuma, T. Hattori, J. Catal. 227 (2004) 367.
[14] K.A. Bethke, H.H. Kung, J. Catal. 172 (1997) 93.
[15] M. Haneda, N. Bion, M. Daturi, J. Saussey, J.-C. Lavalley, D. Duprez, H. Hamada, J. Catal. 206 (2002) 114.
[16] N. Bion, J. Saussey, M. Haneda, M. Daturi, J. Catal. 217 (2003) 47.
[17] K. Shimidzu, J. Shabata, H. Yoshida, A. Satsuma, T. Hattori, Appl. Catal. B 30 (2001) 151.
[18] A. Iglesias-Juez, A.B. Hungría, A. Martínez-Arias, A. Fuerte, M. Fernández-Garcia, J.A. Anderson, J.C. Conesa, J. Soria, J. Catal. 217 (2003) 310.
[19] J. Texter, J.J. Hastrelter, J.L. Hall, J. Phys. Chem. 87 (1983) 4690.
[20] K.I. Hadjiivanov, Catal. Rev. Sci.-Eng. 42 (2000) 71.
[21] A.N. Pestryakov, A.A. Davydov, J. Electron. Spectrosc. Relat. Phenom. 74 (1995) 195.
[22] N.E. Bogdanchikova, V.P. Petranovskii, R. Machorro, Y. Sugi, V.M. Soto, S. Fuentes, Appl. Surf. Sci. 150 (1999) 58.
[23] C. Shi, M. Cheng, Z. Qu, X. Bao, Appl. Catal. B 51 (2004) 171.
[24] W.-S. Ju, M. Matsuoka, K. Iino, H. Yamashita, M. Anpo, J. Phys. Chem. B 108 (2004) 2128.
[25] A.J. Varkey, A.F. Fort, Solar Energy Mater. Solar Cells 29 (1993) 253.
[26] B.G. Ershov, E. Janata, A. Henglein, J. Phys. Chem. 97 (1993) 339.
[27] F.C. Meunier, J.P. Breen, V. Zuzaniuk, M. Osson, J.R.H. Ross, J. Catal. 187 (1999) 493.
[28] Y. Yu, H. He, Q. Feng, H. Gao, X. Yang, Appl. Catal. B 49 (2004) 159.
[29] S. Kameoka, Y. Ukisu, T. Miyadera, Phys. Chem. Chem. Phys. 2 (2000) 367.
[30] T. Baba, H. Sawada, T. Takahashi, M. Abe, Appl. Catal. A 231 (2002) 55.
[31] T. Baba, Y. Abe, Appl. Catal. A 250 (2003) 265.
[32] J. Park, C.G. Jongsma, R. Zhang, S.W. North J. Phys. Chem. A 108 (2004) 10688.
[33] J. Zhang, T. Dransfield, N.M. Donahue, J. Phys. Chem. A 108 (2004) 9082.